



INVESTIGATIONS ON THE SUSCEPTIBILITY TO ATMOSPHERIC-INDUCED STRESS CORROSION CRACKING OF AUSTENITIC STAINLESS STEEL NUCLEAR STRUCTURES

John Wintle¹, Yin Jin Janin², and Stuart Lyon³

¹ Consultant Engineer, Structural Integrity Technology Group, TWI Limited, Cambridge CB21 6AQ, UK (john.wintle@twi.co.uk)

² Mechanical Engineer, Fracture Integrity Management Section, TWI Limited, Cambridge CB21 6AQ, UK (yin.jin.janin@twi.co.uk)

³ AkzoNobel Professor of Corrosion Control, Corrosion and Protection Centre, School of Materials, University of Manchester, Manchester M13 9PL, UK (stuart.lyon@manchester.ac.uk)

ABSTRACT

This paper presents the results of experimental and computational investigations in to the conditions required for the occurrence and the avoidance of atmospheric induced stress corrosion cracking (AISCC) of austenitic stainless steel nuclear structures. The investigation was made on parent and weld material extracted from an intermediate level waste (ILW) nuclear storage container. However, the results are relevant to other stainless steel nuclear structures operating under similar conditions.

The aim of the work is to quantify the combined effects of stress, temperature and humidity on the susceptibility to AISCC from different types of surface salt deposits. The residual stresses associated with the fabrication and welding of ILW containers are characterized by means of a variety of experimental measurements and numerical analyses of the welding. The susceptibility to AISCC was investigated in experiments on welded and parent material specimens loaded under controlled stress conditions in a humidity chamber.

The results show a matrix of conditions where cracking can occur and where it can be avoided. Under very high stress cracking can be observed in a short period of time at temperatures as low as 40°C. Higher temperatures are necessary for cracking to occur at lower levels stress, but the susceptibility to long duration exposure is still uncertain. The paper discusses how the results may influence the fabrication of management of ILW containers and other such structures and the further investigations needed to obtain greater resolution and understanding of long term behaviour.

INTRODUCTION

The work in this paper describes a research collaboration project on AISCC, between TWI and the University of Manchester. The research is relevant to welded austenitic steel structures exposed to airborne salt particles in a humid atmosphere. The specific application of the research was austenitic stainless steel containers used for storing ILW within the UK.

The general assumption is that stress corrosion cracking, including AISCC, of austenitic stainless steels does not occur at temperatures below 60°C. This has now been proven incorrect. Recent published work by Phan (2009) and Cook et al. (2010) has produced AISCC at temperatures as low as 40°C in U-bend specimens of parent material from surface deposited salt particles exposed to a humid atmosphere.

U-bend specimens generate stresses well beyond yield at the apex but do not provide good quantified control over the applied stress or strain. There was therefore a need to determine the threshold for cracking in terms of the stress-temperature combination more accurately. An investigation was proposed with improved control over stress distribution and more detailed analysis of the effect of residual stress on the susceptibility to AISCC. By quantifying the residual stress, it would be possible to

determine the stress threshold for AISCC in both parent and weld specimens. The time at which AISCC can occur is also of practical importance.

In the UK, the current practice is that ILW containers are kept above ground in ventilated storage buildings, often close to coastal areas. These containers will eventually be transferred to a deep underground repository, but this may not occur for many years and the surface storage period has now been extended to up to 150 years. Thus there is a need to maintain structural integrity of these ILW containers during this period to avoid cracking and loss of containment.

During planned storage in ventilated sheds near coastal locations, the exterior of the container will be exposed to the prevailing atmospheric conditions. Contamination comes from dusts, salts, soil, pollution etc., forming a thin layer of electrolyte when sufficient moisture is present. The electrolyte on the metal surface will be affected by temperature and local airflow as well as relative humidity (RH) and these conditions render it susceptible to AISCC.

While the research has been based on material from an ILW container, the results are applicable to a wide range of austenitic stainless steel structures where salt particles can reside on the surface for a prolonged period. These could include corrosion resistant alloys used on some types of reactor plants and reprocessing plants in marine environments.

AISCC

Stress Corrosion Cracking (SCC) is a general term used to describe failures in stressed components that occur by crack propagation under corrosive environments. The requirements for SCC to occur include the presence of (a) a tensile stress, (b) a corrosive environment, and (c) a susceptible material or microstructure. Its occurrence may be preceded by surface corrosion reactions and pitting. Crack growth results from the combined reaction between mechanical stress and corrosion.

Conventionally SCC occurs as a result of the exposure of a metal surface to a flowing or stagnant fluid (gas or liquid) containing corrosive species. AISCC is a particular form of SCC. The corrosive environment is generated by a deliquesced (dampened) salt on a metal surface that forms a layer of electrolyte in the absence of full immersion in aqueous solution, see Figure 1.

A commonly argued mechanism explains SCC as a rupture of the protective passive film leading to the initiation of cracking at the ruptured sites, which are more susceptible to localised corrosion attack. The level of tensile stress in the material generally determines the rate of crack propagation, thus the greater the stress the shorter the expected time to failure (Ferreira et al, 2001). Crack growth tends to occur perpendicular to the principal stress direction although microstructural effects will cause variations in this general trend. Cracks also tend to be branched.

Most studies on conventional SCC are focussed on high-temperature environments, or at least above 60°C, with immersed exposure in a fluid (Szklańska-Smiałowska et al, 1994; Truman, 1994). However, in an early article by Staehle (1976) he noted a few important points, one of which states that SCC is not an inherently high-temperature process. For example, SCC can occur below 0°C in dry hydrogen and at 0°C in aqueous environments; and in other systems which require temperatures above 100 to 200°C. He also argues that a concentrated or aggressive environment is not necessary for SCC to occur.

Current understanding of AISCC is that it occurs when a hygroscopic salt or aerosol particle deposits on a metal surface and starts absorbing moisture from the surrounding atmosphere at a critical RH. The absorption results in a thin layer of saturated salt solution on the metal surface. Localised attack such as pitting or crevice corrosion can then occur.

The major differences between conventional SCC (CSCC) and AISCC are:

- Unlike CSCC, AISCC does not require full immersion or large quantities of corrosive media.
- AISCC is usually triggered by deliquescence of salts that have settled on the component surface, or by capillary action which draws moisture toward inert particles.
- AISCC is dependent on salt type hence making it dependent on RH and temperature.

- AISCC requires long exposure (initiation) times before cracking at ambient temperatures.
- AISCC occurs in atmospheres generally regarded as benign.

Atmospheres are not consistent: the level of RH and contaminants in the air can vary significantly between urban and coastal areas. Stainless steel in coastal areas is more susceptible to AISCC as the air can carry vapour consisting of sea water onto the shore. Urban sites tend to be more polluted with fossil fuel combustion products, which are also corrosive, but chloride is the main aggressive anion.

EXPERIMENTAL TESTING OF ILW CONTAINERS

Container design

The design of a UK ILW container is shown in Figure 2 (NDA, 2008). They are cylindrical drums fabricated from grade 316L and 304L stainless steels welded using TIG welding (TWI, 2002). The containers comprise a circular flat base (316L) nominally 800mm diameter and 2.9mm wall thickness with a shallow up-stand edge that is welded to a cylindrical body nominally 2.3mm wall thickness made from a single cylindrical strake (316L). The upper end of the body is welded to a reducing diameter neck section (316L).

The body has a series of circumferential contours providing added strength against side impact. The top edge of the body is welded onto a flange (304L). The drum lid (316L) of 2.9mm wall thickness also with a welded flange (304L) is sealed onto the drum by bolted outer rings around the flange of the lid. A sintered stainless steel filter element is incorporated in the container lid vents. is not aimed to provide any shielding against radiation. The radioactivity of the ILW is sufficiently low as not to require any shielding.

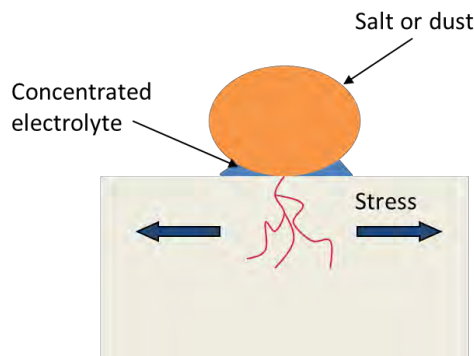


Figure 1. Illustration of AISCC.

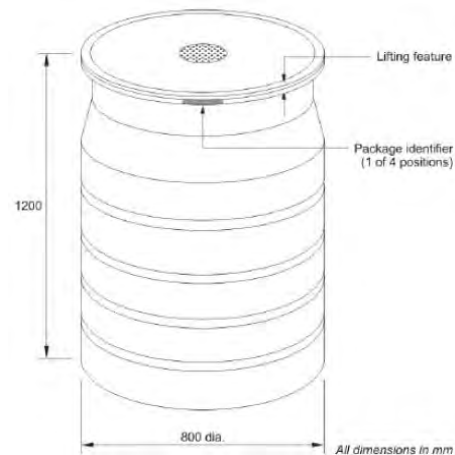


Figure 2. Schematic illustration of an ILW container (NDA, 2008).

Specimen preparation

All AISCC tests were undertaken on specimens machined from the neck and upper body sections of the 500l ILW container. The specimens were in the form of slightly curved longitudinally orientated strips or bars with dimensions of 100mm long x 15mm wide x 2.3mm deep (the full thickness of the container). Some specimens were wholly of parent material whereas others contained the neck-to-body weld across their mid length.

The sides and ends of the specimens were ground to the correct width and length but the top and bottom surfaces and weld areas were left in the as-received condition. One parent specimen was annealed at 1100°C and allowed to furnace cool for 24 hours to reduce residual stresses to a low level. Another parent specimen was etched using a mixture of 8% perchloric acid and 92% glacial acetic acid at 40-45V

to remove a thin surface layer of 100microns. All the specimens were mechanically etched on one end with an alphanumeric identification. They were cleaned in acetone then deionised water to remove all residues and debris from manufacturing and handling.

From this point onwards, all specimens were only handled using powder-free gloves. After cleaning with deionised water, they were kept in a desiccator for at least 24 hours to ensure thorough drying. Biaxial strain gauges were then attached on the bottom (inner) surface in line with the main axes.

External loading of specimens

Specimens to be externally loaded were placed in a jig with adjustable rollers to apply 4-point bending. (Other specimens were retained unloaded as control specimens.) The strain gauges were connected to a converter, a “strain box” which allows strain logging. The strain box converts the electrical resistance detected by the strain gauges into electrical signals from which micro-strain is derived and displayed by the logging software.

The jig was tightened by hand sufficient to lock the specimen securely between the rollers. It was then further tightened to increase displacement of the specimen and the resulting biaxial strain and displacement were measured and recorded. The displacement at mid-length was measured using a displacement gauge. A four-point bend specimen mounted on a jig is shown in Figure 3.

The stress induced by imposed displacement was calculated from measured strains. Displacement was applied to a level of strain sufficient to raise the stress to the measured yield (0.2% proof strain) stress of the parent material i.e. around 400MPa. Both Young’s modulus and proof stress were obtained from the tensile of a longitudinal sample extracted from the ILW container. The straining of these four point bend specimens was performed within the elastic region of the stress-strain curve and was kept as close to the value of proof stress as possible as.

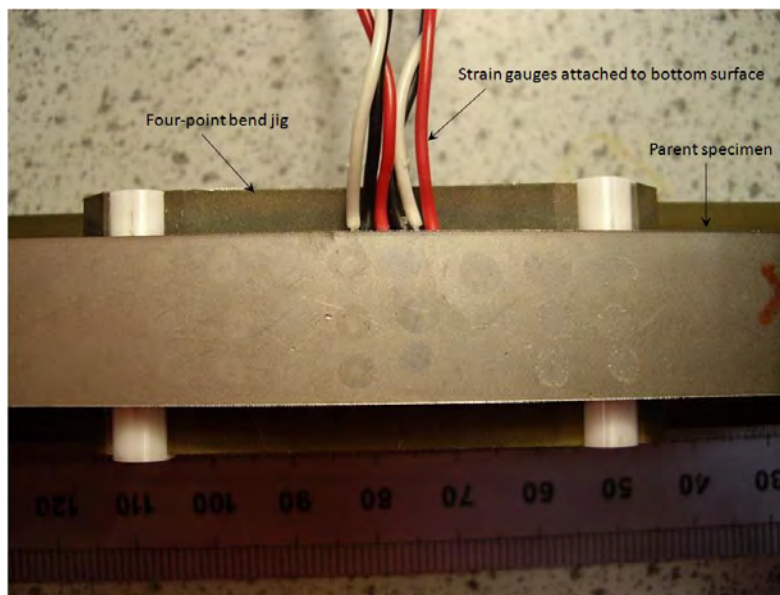


Figure 3. A parent specimen fitted on a four-point bend jig.

Application of the surface salt

Three levels of salt surface density (10, 30 and 100 μgcm^{-2}) were chosen to investigate the relation between surface density and AISCC. Droplets of solution were placed by a pipette on the outer surface of the specimens in an array of positions on the parent material and weld metal. After application of salt

solution, the specimens were dried in a desiccator for at least 24 hours so that the droplets evaporated leaving the salt on the surface.

Three different types of salt were used in this investigation: sodium chloride, magnesium chloride and synthetic sea salt. The droplet diameters (and hence surface areas formed upon evaporation) were all consistent. The pipette dispensed droplets of $5 \pm 0.1 \mu\text{l}$ measured as approximately $3 \pm 0.1 \text{mm}$ in diameter. If the surface area of droplet is defined as A and the amount of salt contained in a $5 \mu\text{l}$ droplet is m , then for a surface density of $100 \mu\text{gcm}^{-2}$:

$$100 \mu\text{gcm}^{-2} = \frac{m}{A} \quad (1)$$

A $5 \mu\text{l}$ droplet with a diameter of 3mm will give surface area A of 0.070686cm^2 and thus contains $m = 7.0686 \mu\text{g}$ of salt in the $5 \mu\text{l}$ droplet. Salt amounts for other deposition rates can be determined simply by ratio. Finally, in order to calculate the quantity of salt added to the stock solution in order to achieve the required deposition rate, the chemical formula (and molecular weight) of the species added is required; for example: sodium chloride is NaCl (58.5g mol^{-1}) while magnesium chloride is $\text{MgCl}_2 \cdot 6\text{H}_2\text{O}$ (203.31g mol^{-1}). The concentration of solutions required to achieve the desired surface densities are tabulated in Table 1.

The list of specimens is tabulated in Tables 2 and 3. There were seven 4-point bend specimens in total: three of parent material, two of weld metal, one of annealed parent material and one of etched parent material.

Table 1: Preparation of salt solution with different loading densities.

Salt type	Amount of salt required per litre, g/l		
	$100 \mu\text{g/cm}^2$	$30 \mu\text{g/cm}^2$	$10 \mu\text{g/cm}^2$
Sodium chloride	1.4137	0.4241	0.1413
Magnesium chloride	3.0179	0.9054	0.3018
Synthetic sea salt	1.4137	0.4241	0.1413

Table 2: List of 316L 4-point bend specimens.

	Material	Condition	Synthetic seawater†	Magnesium chloride, $\mu\text{g/cm}^2$			Sodium chloride, $\mu\text{g/cm}^2$		
				100	30	10	100	30	10
P1	parent	As-received	X	X	X	X	X	X	X
P2	parent	As-received	X	X	X	X	X	X	X
P3	parent	As-received	X	X	X	X	X	X	X
W1	weld	As-received	X	X	X	X	X*	X*	X*
W2	weld	As-received	X	X	X	X	X*	X*	X*
P9	parent	Annealed	X	X	X	X			
P12	parent	Etched	X	X	X	X			

*Reapplied with magnesium chloride and synthetic seawater solutions only as the first application of NaCl did not promote corrosion

† Diluted to $100 \mu\text{gcm}^{-2}$, $30 \mu\text{gcm}^{-2}$ and $10 \mu\text{gcm}^{-2}$

Control specimens

Control specimens are small unloaded specimens which were prepared from the as-received ILW container. Six control specimens were deposited with sodium chloride, magnesium chloride and synthetic seawater salt deposits. The specimens were placed in the environmental chamber but not loaded in four-

point bending so as to investigate the effect of residual stress alone. A seventh control specimen which had been annealed was also placed in the humidity chamber.

Table 3: List of 4-point control specimens.

	Material	Condition	Synthetic seawater†	Magnesium chloride, $\mu\text{g}/\text{cm}^2$			Sodium chloride, $\mu\text{g}/\text{cm}^2$		
				100	30	10	100	30	10
U0	weld	Annealed							
U1	weld	As-received	X						
U2	weld	As-received		X	X	X			
U3	weld	As-received					X	X	X
U4	weld	As-received	X						
U5	weld	As-received		X	X	X			
U6	weld	As-received					X	X	X

Environmental chamber exposure

The environmental chamber used was a CTS -40/60 model manufactured by Climatic Testing System Inc. The chamber was visited on a daily basis whenever possible to ensure correct functioning and intermittent temperature checks were carried out using a calibrated thermometer.

The externally loaded and control specimens were kept at 40°C and 40%RH for the first nine months (March to December 2010). As there had been no cracking at the end of this time, the decision was taken to raise the temperature to 80°C, with a corresponding reduction in RH to 27%RH. The DRH of magnesium chloride at 80°C is 26%RH. The same specimens remained in the chamber and some additional welded specimens loaded with magnesium chloride and sea salt droplets were added. These conditions were maintained for a year until December 2011.

The decision to increase the temperature was taken because observations of highly plastically strained U-bend specimens in previous experiments at Manchester University suggested that it might take too long before cracking would occur in the four-point bending specimens loaded to yield. It took around three months before cracking occurred in U-bend specimens in Manchester (Phan, 2009; Cook et al, 2010). It seemed reasonable enough to accelerate the exposure testing by increasing the temperature and decreasing the RH to still be above the DRH of magnesium chloride and sea salt, which has a high proportion of magnesium chloride, hoping it would produce some visible cracks, even though the reduced RH would be below the DRH of sodium chloride where no cracking would be expected.

In December 2011, the temperature was decreased and RH increased to values intermediate between the first and second testing conditions: that is the third testing condition was at 60°C and 32%RH. This condition was maintained from December 2011 until the end of the experimental programme (May 2012). Table 4 summaries the testing conditions and duration.

When the temperature was increased at the second phase to 80°C, the logging from the strain gauges was discontinued as the gauges were affected by high temperature and gave false readings. It was therefore assumed that the external load was maintained and there was no creep in the jigs.

Surface examination of specimens

The areas under the salt deposits on the specimens were examined approximately twice a month using an optical microscope to determine if any corrosion, pits or cracks were present. Photographs were taken periodically and the digital images stored and compared with prior images. Changes between

corresponding images were tracked. Further analysis was conducted using an Olympus LEXT OLS4000 3D confocal laser microscope for 3D scanning to determine the depth of the pits.

One parent material specimen (labelled Parent 2) was removed from the chamber in February 2011 and examined by scanning electron microscopy. Images were taken before and after corrosion product removal. Energy dispersive spectroscopy (EDX) surface analyses were also conducted of a location deposited with sea salt.

Table 4: List of specimens and their associated testing period in hours.

	Loading	Condition	No. of hours at 40°C, 40%RH	No. of hours at 80°C, 27%RH	No. of hours at 60°C, 32%RH
P1	4-point bend	Parent	6480	2880	NA
P2	4-point bend	Parent	6480	2880	NA
P3	4-point bend	Parent	6480	2880	NA
W1	4-point bend	Weld	6480	6480	3600
W2	4-point bend	Weld	6480	6480	3600
P9	4-point bend	Parent Annealed	NA	2160	3600
P12	4-point bend	Parent Etched	NA	2160	3600
U0	Unloaded	Annealed	6480	6480	3600
U1	Unloaded	Weld	6480	6480	3600
U2	Unloaded	Weld	6480	6480	3600
U3	Unloaded	Weld	6480	6480	3600
U4	Unloaded	Weld	6480	6480	3600
U5	Unloaded	Weld	6480	6480	3600
U6	Unloaded	Weld	6480	6480	3600

RESULTS

General observation

During the first nine months, the specimens underwent exposure at 40°C and 40% RH. Rust coloured corrosion products (discoloured region on specimens) were observed beneath precipitated salt crystals of magnesium chloride and sea salt only (not sodium chloride). The presence of pits or cracks could not be confirmed, because the surface was masked by corrosion products and any pitting or cracking present was too small to be detected under the optical microscope available.

During the first phase of exposure at 40%RH and 40°C, the MgCl₂ droplets of 10 and 30µg/cm² surface density had less severe corrosion than those of 100µg/cm². The corrosion associated with the sea salt droplets appeared more severe than that for the MgCl₂. The area covered by corrosion product in a sea salt deposit is wider than that of magnesium chloride. Corrosion appeared in a random manner over the area within the perimeter of each droplet.

After increasing the temperature to 80°C and decreasing the RH to 27% in the second phase, the corrosion discolouration of the metal surfaces spread beyond each droplet. After one month pits up to 260µm across were observed on both weld and parent material specimens (externally loaded and control) under the magnesium chloride and sea salt droplets (not sodium chloride) of all three surface densities. While the number of pits increased in subsequent months, the pit diameters did not change appreciably over the remaining course of the experiment when examined twice a week.

Corrosion products were present in the pits. Some pits also appeared to have shiny surfaces. Cracks up to 100 μm long and 20 μm wide were observed in some of the pits on the externally loaded specimens but not in the pits on the control specimens. The number of cracks increased in subsequent months but it is not clear whether this was directly associated with the number of pits. Table 9 shows a summary of the AISCC susceptibility for the different specimens.

At the third phase, the conditions were altered again to 60°C and 32%RH. The original specimens remained and new specimens were included. During the five months to date, there have been no observable changes to the numbers and sizes of the pits and cracks in the original specimens. The new specimens have become corroded with the exception of the specimen that was etched, where no corrosion is evident. This is believed to be because pickling removes the surface inclusions such as manganese sulphide (MnS). MnS inclusions are commonly the sites of localised attack where pits initiate. Thus the pitting tendency for the pickled surface should be reduced.

Examination of surface pits and cracks

As little was observed in the first phase, the same specimens were kept in the humidity chamber and proceeded into the second phase with an increase in temperature and decrease in RH.

The morphology of specific pits and cracks were examined under a SEM before and after the surface had been cleaned of corrosion product. The quadrant back scattering detector (QBSD) confirms the visual observation mentioned in the previous section that the size of the pits was approximately 260microns across.

Left image of Figure 4 shows two suspected cracks as indicated by arrows. It also shows regions labelled (1), (2), (3) and (4) at which EDX has been conducted to analyse the chemical composition of the surface. The qualitative EDX analysis of regions labelled (1) and (2) show peaks for oxygen and chlorine which is a clear indication that it is a corrosion product. The EDX analysis of the region labelled (3) shows peaks for Fe and Cr. The relative height of the peak of O is much lower than the two previous analyses. Only Na and Cl are detected in region labelled (4). Right image of 4 confirms the presence of cracks under salt droplet. There are visible cracks in at least three pits.

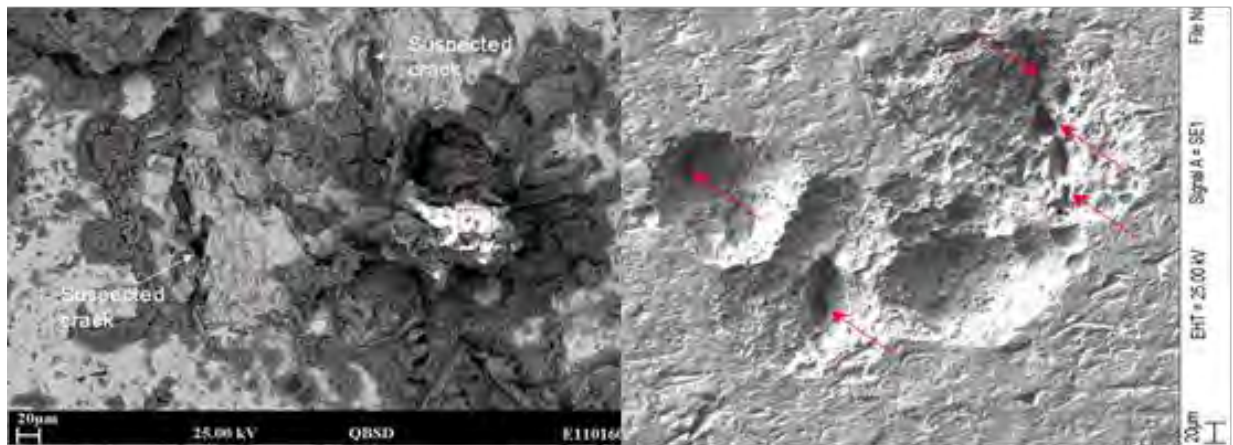


Figure 4. Morphology of specific pits and cracks before clean-up (Left image) and after clean-up (Right image) with arrows indicating cracks.

The observations at the end of the third stage exposures showed no significant difference from the second phase. Corrosion was observed on weld specimens for both magnesium chloride and sea salt deposits. The pitting on the control specimens inherited from the second phase did not seem to have advanced. The etched specimens did not pit. The annealed 316L specimen only showed light corrosion at locations deposited with synthetic seawater.

The corrosion products under all salt droplets are the result of the deliquescence chlorides of sodium, magnesium or calcium (from sea salt) in the humid atmosphere of the chamber. Storage of the specimens in a desiccator prior to the test did not produce any corrosion. The DRH of both MgCl₂ and CaCl₂ is approximately 30-35%RH at room temperature, 26-31%RH at 80°C and 31-34%RH at 60°C.

No corrosion was observed under any of the NaCl droplets which have a deliquescence threshold of about 75%RH. However, corrosion under synthetic seawater droplets was observed to occur in a random pattern probably due to the uneven precipitation of other salts present in the seawater mixture at the low RH (i.e. mainly sodium chloride but also calcium sulphate etc.). There is a suggestion from the NDA to keep the RH of storage buildings below 70%RH. But the aerosol particles present in the atmosphere are rarely composed of a single pure element but of a mixture of a few constituents such as salts of nitrates and sulphates.

The effect of other less soluble precipitates on AISCC susceptibility remains undetermined but the presence of other salts in the salt mixture influences the DRH. Tang and Munkelwitz (1993) showed that the DRH of a salt mixture is lower than the minimum DRH of each component:

$$DRH(salt_1, salt_2, \dots, salt_n) < \min\{DRH_{salt_1}, DRH_{salt_2}, \dots, DRH_{salt_n}\} \quad (2)$$

The DRH of the mixture does not have a unique value. It is a function of mixture composition and is commonly known as the Mutual Deliquescence RH (MDRH) or eutonic point. At MDRH the aqueous phase is saturated with respect to all components in the mixture, so it is the only RH at which an aqueous solution can coexist with a precipitate consisting of all the aerosol salts.

DISCUSSION

A summary of the conditions where AISCC has been observed and where it did not occur in the tests that have been carried out is shown in Table 5. It can be seen that there is increasing susceptibility to AISCC with increasing temperature and stress. While TWI observed cracking at 400MPa and 80°C, it is more significant that no cracking was observed at either 60°C or 40°C at this stress level or at 170MPa or zero stress at 80°C within 6 months exposure. However, the “incubation period” of nine months at 40°C would have an effect on the cracking at 80°C.

Table 5: The conditions where AISCC has been observed and where it did not occur in the tests that have been carried out

Temperature, °C	U-bend tests (Phan, 2009; Cook et al., 2010)	4-point bend tests		Control specimens
		As-received	Annealed	As-received
	$\sigma > 400\text{MPa}$	$\sigma \approx 400\text{MPa}$	$\sigma \approx 170\text{MPa}$	$\sigma \approx 0\text{MPa}$
80	✓	✓	✗	✗
60	✓	✗	✗	✗
40	✓	✗✗	✗✗	✗✗
20	No data	No data	No data	(✗)

✓: Cracking occurred within 3 to 4 months; ✗: No cracking before 6 months; ✗✗: No cracking after 9 months; (✗): No cracking, assumed result

These results suggest that there may be a level of stress between 400MPa and 170MPa below which AISCC does not occur from exposure at 80°C. Similarly there may be a temperature between 80 and 60°C below which AISCC does not occur at a stress of 400MPa. Further, there may be a stress between 400MPa and that reached in the U-bend tests (unknown but in excess of 400MPa) where cracking may not occur at 60 and 40°C.

In all these cases there is a strong possibility that AISCC is time dependent and that cracking could occur over much longer exposure periods. The occurrence of AISCC is thus a complex function of stress, temperature and time that has not yet been established. It is clear that further experiments are necessary to provide more detail within the field of the experimental variables. Cracking has not been observed in weld metal. This is believed to have been prevented by the ferrite network present in the weld metal.

One of the major concerns for the safety of ILW containers is their structural integrity during surface storage in a repository building for 150 years prior to disposal by burial and backfill. Recent studies and experience of failures have shown that AISCC can occur from airborne salt particles under ambient environmental conditions. The results of this work provide insight for the avoidance of AISCC of ILW containers through understanding the effects of the container manufacturing process and the design and environmental management of storage buildings.

CONCLUSION

This work has shown that atmospheric-induced stress corrosion cracking of stainless steels can occur under a surface salt within a few weeks of exposure at 80°C in a humid atmosphere where loaded under controlled conditions to a stress of 400MPa, providing the RH of the atmosphere is equal to or greater than deliquescence relative humidity of the salt.

Cracking did not occur within nine months under these conditions when the temperature was 40°C. No difference in racking behavior was observed between parent and autogenous weld metal. Given that cracking was observed in U-bend specimens after a short period at stress levels well in excess of 400MPa, further work is necessary to determine more accurately the stress level at which cracking will occur at lower temperatures and whether the exposure time has an effect. As residual stresses greater than 400MPa have been measured in the welds of an ILW container, future work should be directed at providing insight into the conditions and measures required to avoid cracking of containers in storage.

REFERENCES

- Cook, A., Stevens, N. P. and Duff, J. (2010). "Atmospheric corrosion of nuclear waste containers," *DIAMOND'10 Conference Decommissioning, Immobilisation and Management of Nuclear Waste for Disposal*, Manchester.
- Ferreira, M. G., Goodlet, G., Faty, S., Simoes, A. M. and da Cunha Belo, M. (2001). "Influence of the temperature of film formation on the electronic structure of oxide films formed on 304 stainless steel," *Electrochimica Acta*, 46, 3767-3776.
- NDA. (2008). *Waste package specification and guidance document WPS/630: Guidance on environmental conditions during storage of waste packages*.
- Phan, D. (2009). "Atmospheric-Induced Stress Corrosion Cracking of Austenitic Stainless Steel," PhD thesis, University of Manchester, Manchester, UK.
- Staehle, R. W. (1976). "Stress corrosion cracking (and corrosion fatigue)," *Materials Science and Engineering*, 25, 207-215.
- Szklarska-Smialowska, Z., Rebak, P., Skulte, P. and Xia, Z. (1994). "Pitting and Stress Corrosion Cracking Susceptibility of Low Alloy Steel (SA grB) in Steam Generator Conditions," *Corrosion*, 50, 279-289.
- Tang, I. N. and Munkelwitz, H. R. (1993). "Phase transformation and growth in the atmosphere," *Journal of Applied Meteorology*, 33, 791-794.
- Truman, J. E. (1994). Chapter 3.3: Stainless steels. In *Corrosion Volume 3*. Butterworth-Heinemann.
- TWI Ltd. (2002). "Best practice guide: Welded joint design and manufacture for stainless steel," containers. *Nirex Ref No. 388940*.